

# Semiclassical Wave Packet Dynamics with Electronic Structure Computed on the Fly: Application to Photophysics of Electronic Excited States in Condensed Phase

Alfredo E. Cárdenas, Roman Krems, and Rob D. Coalson\*

Department of Chemistry, University of Pittsburgh, Pittsburgh, Pennsylvania 15260

Received: June 1, 1999; In Final Form: July 28, 1999

Many semiclassical wave packet propagation methods require only local potential energy surface information in order to update a Gaussian wave packet over a short time interval. These data, which include the evaluation of the potential energy at the instantaneous configuration space center of the wave packet, plus the gradient vector and Hessian (second derivative) matrix at the same configuration, can be generated efficiently by extant electronic structure packages. This leads to an algorithm for propagating semiclassical Gaussian wave packets using electronic structure data computed “on the fly” in the course of the propagation. The feasibility of such a strategy for condensed phase systems is demonstrated by using it (with an appropriate approximate level of electronic structure theory) to calculate Franck–Condon absorption and emission spectra of *all-trans* 1,3,5,7-octatetraene in the gas phase, and in both chloroform and methanol solvents. Good agreement with the corresponding experimentally measured spectra is obtained.

## 1. Introduction

The problem of computing reliable dynamical signatures (spectra, scattering cross sections, reaction rate constants, etc.) of condensed phase quantum systems remains challenging for two basic reasons. First, there are severe practical difficulties in propagating wave packets<sup>1</sup> that describe the quantum motion of the nuclear coordinates. Second, a quantum dynamics calculation is ultimately only as good as the potential energy surfaces upon which it is based, yet high-level *ab initio* electronic structure calculations<sup>1</sup> can only be carried out for small isolated molecule systems. The task of generating such surfaces for large molecules or for probe molecules that interact with a condensed phase environment is a daunting one. The situation is particularly bleak when the relevant quantum dynamics occurs on electronically excited potential energy surfaces (e.g., in many photoinduced processes), since it is much more difficult to compute accurate excited electronic potential surfaces than ground state properties.

For systems with only a few degrees of freedom (ca. 5 or less), it is possible to calculate and store global potential energy surfaces, i.e., ones which span the full relevant range of each nuclear coordinate, via *ab initio* electronic structure theory. Once the relevant potential energy surface (PES) is stored, nuclear coordinate wave packets can be propagated on it using exact numerical grid and/or basis set technology. For systems much larger than this, construction of a global PES is not feasible. Of course, in many situations a global potential surface is not strictly required. For example, if the nuclear coordinates can be treated classically, one needs only to determine the gradient of the potential surface at the *instantaneous* configuration of the nuclear coordinates in order to update this configuration by a small time step. The gradient has to be recomputed at each time step, but for a system with many nuclear coordinates (e.g. a condensed phase system), this is vastly preferable to attempting to construct a global multidimensional potential surface. Indeed, this strategy, namely, using electronic structure methodology to determine the potential energy gradient at the instantaneous

nuclear coordinate configuration coupled with Newton’s equations of classical mechanics, has proven extremely useful in recent years.<sup>2</sup> The central issue we wish to consider here is to what extent the concept of on the fly determination of potential energy surfaces can be extended to enable *quantum mechanical* propagation of the nuclear coordinates.

A nuclear coordinate wave packet is localized in some region of space at a particular time, and it is only necessary to know the potential energy surface in that region (i.e., where the wave packet has nonzero amplitude) to update it by a small time step according to the time-dependent Schrödinger equation. This property does not necessarily provide any practical advantage: one would still need to map out (by quadrature) the potential energy surface in the appropriate region of multidimensional coordinate space, and then update the wave packet on the corresponding multidimensional coordinate grid. However, if the wave packet is well localized, several features conspire to make the prospect of wave packet dynamics with potential surfaces computed on the fly much more attractive. A narrow Gaussian wave packet remains Gaussian in time (until it broadens to a critical width; cf. below). This allows the utilization of Heller’s Gaussian wave packet dynamics (GWD) algorithm to propagate *multidimensional* wave packets.<sup>3</sup> GWD requires at most a quadratic Taylor series expansion of the potential energy surface around the instantaneous center of the wave packet (the “thawed Gaussian approximation”).<sup>4</sup> Thus, a call to the electronic structure (ES) part of the algorithm need only provide at each step the value of the potential energy at the current nuclear coordinate configuration, plus the gradient and Hessian (second derivative matrix) at that configuration. These quantities are readily produced by standard electronic structure programs/software packages. With this minimal amount of “local” potential energy information it is possible to update the Gaussian wave packet representing the nuclear coordinate wave packet state by a small time step, and then repeat the process again. Indeed, we note that in certain situations (e.g., if the width of the nuclear coordinate wave packet is *very* small) a simpler approximation to the nuclear coordinate wave packet

motion, namely the frozen Gaussian approximation,<sup>5</sup> suffices. In this case second derivative (Hessian) ES data is not required, and the strategy reduces to the one used to propagate the nuclear coordinates classically (vide supra).<sup>6</sup>

Of course, the condition that the nuclear coordinate wave packet remains narrow imposes restrictions on the range of dynamical processes that can be treated by the strategy proposed above. For the general case of anharmonic potential energy surfaces, an initially narrow wave packet will eventually spread until the potential surface cannot be represented by a quadratic form in the entire spatial region where the wave packet is nonzero.<sup>8</sup> How long it takes to reach this point depends on the details of the shape of the potential surfaces, mass of the atoms, initial conditions, etc. A variety of applications of the technique indicate that many dynamical processes on a subpicosecond time scale can be successfully treated using the Gaussian approximation of the nuclear coordinate wave packet states.<sup>9–13</sup> It is this class of processes which we focus on here.<sup>14</sup>

In the present work we combine Gaussian wave packet dynamics with potential energy surfaces computed on the fly to study the electronic absorption and emission spectra of *all-trans* octatetraene, both as an isolated molecule and immersed in a liquid solvent. Octatetraene is the shortest polyene that shows clear emission spectra.<sup>19–21</sup> It is composed of 18 atoms, and hence 48 vibrational coordinates. We treat their quantum dynamical evolution motion via Gaussian wave packet dynamics, while the relevant 48-dimensional PES's are computed on the fly using Warshel's semiempirical QCFF/PI electronic structure code.<sup>22,23</sup> We are able to reproduce well-resolved experimental gas phase Franck–Condon spectra using this procedure. We then model the analogous spectra for octatetraene in room temperature polar solvents, specifically chloroform and methanol. Because solvent relaxation takes place on a multi-picosecond time scale while the relevant nuclear wave packet dynamics contributing to Franck–Condon absorption/emission spectra lasts less than 100 fs, we employ a static solvent model; i.e., the solute (octatetraene) motion takes place in the potential field generated by a static solvent configuration. (This external potential is added to the internal Coulombic interactions of the nuclei and electrons of the octatetraene molecule in the computation of potential energy surfaces using QCFF/PI). We average over solvent configurations selected from a classical equilibrium molecular dynamics simulation to obtain a prediction for the observed condensed phase octatetraene spectrum. Good agreement is found with experimental measurements. Not only are solvent-induced shifts of the absorption and emission bands successfully accounted for, but so are the shapes of the bands. The latter are altered by solvent broadening, but nevertheless retain some vibrational structure. The ability of the methodology utilized here to account for vibronic structure justifies the effort of propagating nuclear coordinate wave packets, and the accuracy of the results compared to experiment demonstrates the utility of performing detailed electronic structure calculations to obtain the required potential energy surfaces.

The outline of the paper is as follows. In section 2 we present methodological details. Section 2.1 briefly reviews the QCFF/PI electronic structure method, and the modifications needed to treat the influence of an external potential energy field (to be provided by electrostatic and nonbonded interactions of the solute molecule with surrounding solvent molecules). In section 2.2 we discuss the classical MD simulations used to generate solvent configurations. In section 2.3 we summarize the GWD method for quantum mechanical propagation of the vibrational

coordinates of the solute molecules, and the procedure used to extract Franck–Condon spectra from this wave packet dynamics. In section 3 we present results for calculated electronic absorption and emission spectra of gas phase octatetraene and the analogues of these spectra for an octatetraene molecule in chloroform and methanol solvents. Direct comparison with experiment is made. Section 4 contains concluding remarks.

## 2. Methodological Details

**2.1. Semiempirical Electronic Structure USING QCFF/PI.** Consider a single solute molecule immersed in a liquid solvent. For a given configuration of solute nuclei and solvent atoms, the Hamiltonian for the electrons of the solute is

$$\hat{H} = \hat{H}_{\text{mol}} + \hat{H}_{\text{sol}} + \hat{H}_{\text{mol/sol}} \quad (1)$$

where  $\hat{H}_{\text{mol}}$  is the quantum mechanical Hamiltonian of the solute (in atomic units):

$$\hat{H}_{\text{mol}} = -\frac{1}{2} \sum_i^n \nabla_i^2 + \sum_{i>j}^n \sum_{ij} \frac{e^2}{r_{ij}} - \sum_i^n \sum_{\alpha}^N \frac{eZ_{\alpha}}{r_{i\alpha}} + \sum_{\alpha}^N \sum_{\beta>\alpha}^N \frac{Z_{\alpha}Z_{\beta}}{R_{\alpha\beta}} \quad (2)$$

Here  $i$  labels the solute electrons ( $n$  in all) and  $\alpha$  the solute nuclei ( $N$  in all);  $r_{ij}$  is the distance between electrons  $i$  and  $j$  and  $R_{\alpha\beta}$  the distance between nuclei  $\alpha$  and  $\beta$ .  $Z_{\alpha}$  is the atomic number of nucleus  $\alpha$  and  $e$  the magnitude of the electron charge. Of the other terms in eq 1,  $\hat{H}_{\text{sol}}$  is the classical Hamiltonian for the solvent (specified in section 2.2) and  $\hat{H}_{\text{mol/sol}}$  is the interaction Hamiltonian that describes the interaction between the solute and the solvent, namely:

$$\hat{H}_{\text{mol/sol}} = - \sum_i^n \sum_k^M \frac{eq_k}{r_{ik}} + \sum_{\alpha}^N \sum_k^M \frac{Z_{\alpha}q_k}{R_{\alpha k}} + \sum_{\alpha}^N \sum_k^M \epsilon_{\alpha k} \left( \frac{\sigma_{\alpha k}^{12}}{R_{\alpha k}^{12}} - \frac{\sigma_{\alpha k}^6}{R_{\alpha k}^6} \right) \quad (3)$$

In this equation the solvent atoms are labeled by  $k$  ( $M$  atoms in all),  $q_k$  is the charge on solvent atom  $k$ ,  $r_{ik}$  is the distance between solute electron  $i$  and solvent atom  $k$ ,  $R_{\alpha k}$  is the distance between solute nucleus  $\alpha$  and solvent atom  $k$ , and  $\epsilon_{\alpha k}$  and  $\sigma_{\alpha k}$  are Lennard-Jones parameters. Clearly, the first two terms in eq 3 account for electrostatic interactions between the (partial) charges on the solvent atoms and the electrons and nuclei of the solute molecule, while the third term accounts for short-range van der Waals forces between solute and solvent atoms.

To calculate the electronic absorption and emission spectra of octatetraene, we require equilibrium geometries and potential energy surfaces for the ground and the first two excited states. Simple MO theories can be used to describe the ground state  $1^1A_g$  and the second excited state  $1^1B_u$ . This corresponds to the  $|\text{HOMO}\rangle \rightarrow |\text{LUMO}\rangle$  transition. To describe the first excited state  $2^1A_g$  it is necessary to use configuration interaction with double excitations, since this state is a mixture of single ( $|\text{HOMO} - 1\rangle \rightarrow |\text{LUMO}\rangle$  and  $|\text{HOMO}\rangle \rightarrow |\text{LUMO} + 1\rangle$ ) and double (mainly,  $|\text{HOMO}, \text{HOMO}\rangle \rightarrow |\text{LUMO}, \text{LUMO}\rangle$ ) excitations. It is possible to perform ab initio calculations for the octatetraene molecule, but our “structure on the fly” method requires many of these calculations to evaluate the potential energy surfaces at the center of the wave packet during its time propagation. For this reason, we have chosen to employ a semiempirical technique to determine the electronic structure of the molecule, specifically the QCFF/PI method developed by Warshel and others with single plus double excited configurations included.<sup>22,23</sup> This model describes the  $\sigma$  electrons with

an empirical potential and the  $\pi$  electrons via a semiempirical quantum-mechanical calculation comprising of self-consistent field plus configuration interaction components. The QCFF/PI program has proven reliable for computing ground and excited states of gas phase polyenes and their associated optical/UV spectra,<sup>23</sup> and has the additional advantage that from a single electronic eigenfunction (obtained by solving the electronic Schrödinger equation at a particular nuclear coordinate configuration) the first and second derivatives with respect to the Cartesian positions of the atoms at that nuclear configuration can be calculated analytically (hence rapidly). These derivatives are needed in order to evolve the nuclear coordinate dynamics using GWD techniques. As noted above (and discussed further below), the QCFF/PI program has been modified to include an additional term in the diagonal elements of the Fock matrix to take into account the electrostatic influence of the partial charges of the solvent molecules on the electronic structure of the solute molecule. Specifically, the Fock matrix under the influence of the solvent can be written as<sup>24,25</sup>

$$F_{ii} = F_{ii}^0 - \sum_k \sum_l \left\langle \varphi_i \left| \frac{eq_l}{r_{kl}} \right| \varphi_i \right\rangle$$

$$F_{ij} = F_{ij}^0 \quad (4)$$

Here  $F^0$  is the Fock matrix of the isolated solute, expressed in a basis of orthogonalized atomic orbitals  $\varphi_i$ . The diagonal Fock matrix elements are modified by the indicated correction terms which reflect electrostatic interactions of the solute electrons with the charges on the solvent atoms according to the first term in  $\hat{H}_{\text{mol/sol}}$ . (The second and third terms in  $\hat{H}_{\text{mol/sol}}$  do not depend on solute electronic coordinates and can be treated as an external field and added directly to the total energy.) The one-electron integrals associated with the interaction Hamiltonian are evaluated analytically using the appropriate expressions for Slater orbitals.<sup>26</sup> The van der Waals parameters used in this calculation are the same ones used in the molecular dynamics calculation detailed below.

**2.2. Classical MD of the Solvent.** For an isolated octatetraene molecule, the QCFF/PI program can be used to evaluate the PES at any atomic configuration. However, when this molecule is immersed in a condensed phase environment, the relevant PES is modified by the presence of the surrounding molecules of the bath. In particular, if the solvent molecules are polar, the electrostatic interaction of the partial charges of these molecules will significantly affect the electronic structure of the polyatomic molecule. This effect can be accounted for by calculating the Coulombic potential in the region of the solute atoms generated by the partial charges present in the solvent. The electric potential field generated by the solvent charges modifies the diagonal elements of the Fock matrix of the molecule (cf. eq 4), and this modification perturbs the potential energy surfaces of the molecule. To incorporate such perturbations we take advantage of the fact that the dynamical time scale for the absorption correlation function is  $<100$  fs, while the typical time scale for rotational relaxation of polyatomic molecules in a liquid phase can be several picoseconds. Therefore, the effects of the solvent can be treated in the “static limit”, i.e., the configuration of the solvent is frozen, nuclear wave packet dynamics on the molecular potential energy surface perturbed by that solvent configuration is computed (details are given in section 2.3), and an average is taken over configurations selected from a thermal equilibrium ensemble to get the condensed phase spectrum. For a liquid solute–solvent system at room temper-

ature, the equilibrium configurations of the (room temperature) solvent can be sampled via classical molecular dynamics (MD) simulations.

We performed MD simulations using the AMBER<sup>27</sup> force field, according to which the total potential energy function for the ensemble of solvent molecules has the form

$$E_{\text{total}} = \sum_{\text{bonds}} K_r (r - r_{\text{eq}})^2 + \sum_{\text{angles}} K_\theta (\theta - \theta_{\text{eq}})^2 + \sum_{\text{dihedrals}} \frac{V_n}{2} [1 + \cos(n\phi - \gamma)] + \sum_{i < j} \left[ \frac{A_{ij}}{R_{ij}^{12}} - \frac{B_{ij}}{R_{ij}^6} + \frac{q_i q_j}{\epsilon R_{ij}} \right] \quad (5)$$

(The definitions of the various force field parameters can be found elsewhere.<sup>27</sup>) For the solvents studied, chloroform and methanol, a rectangular box of solvent molecules was generated (containing 787 and 633 solvent molecules in the cases of chloroform and methanol, respectively). We employed a flexible all-atom model for the molecules using force fields parameters developed as part of the AMBER package.<sup>28,29</sup> The molecular dynamics simulations were performed using explicit image periodic boundary conditions with a time step of 0.5 fs and a temperature of 300 K. We first calculated molecular dynamics of the solvent alone to ensure that solvent properties such as the bulk density were reproduced for the force field parameters chosen for the simulations. Then one molecule of octatetraene was introduced into the solvent box and an MD simulation was performed on the solvent/solute system, keeping the solute rigid (freezing internal vibrations) for the purposes of the simulation. After equilibrating at 1 atm, constant volume dynamics was carried out and we generated multiple sets of solvent configurations separated by 1 ps. For absorption spectrum calculations, the equilibrium geometry and partial charges of octatetraene in the ground electronic state were used in the molecular dynamics simulations. For emission spectrum calculations, the geometry and charges for the  $2^1A_g$  state were used.

**2.3. Nuclear Coordinate Wave Packet Evolution via Gaussian Wave Packet Dynamics and the Extraction of Vibronic Spectra.** As discussed above, to calculate quantum nuclear coordinate evolution on general multidimensional potential energy surfaces it is necessary to use approximate techniques. One such technique is Gaussian wave packet dynamics (GWD), which has been extensively utilized in the past to produce rapid and reliable results for nuclear dynamics on the scale of a picosecond or shorter.<sup>9–13</sup> The general Gaussian wave function for a  $D$ -dimensional system at time  $t$  with spatial coordinate  $\vec{x}$  is

$$\phi(\vec{x}, t) = \exp[i[(\vec{x} - \vec{x}_t) \cdot A_t \cdot (\vec{x} - \vec{x}_t) + \vec{p}_t \cdot (\vec{x} - \vec{x}_t) + \gamma_t]] \quad (6)$$

where  $A_t$  is a  $D \times D$  complex symmetric matrix,  $\vec{x}_t$  and  $\vec{p}_t$  are real  $D$ -dimensional vectors specifying the position and momentum of the center of the wave packet, and  $\gamma_t$  is a complex phase/normalization parameter.

The equations of motion governing the time evolution of the parameters in this Gaussian wave packet depend only on local information about the potential energy surface near the center of the wave packet. Specifically, frozen Gaussian approximation (FGA) wave packet dynamics requires only the gradient of the potential surface at the position space center of the wave packet.<sup>5</sup> Thawed Gaussian approximation (TGA) dynamics also requires second derivative information as input.<sup>4</sup>



Covalently bound molecules usually occupy the ground vibrational state of the ground electronic PES prior to photoexcitation, because typically the vibrational quantum is much larger than  $k_B T$  ( $k_B$  is Boltzmann's constant,  $T$  the absolute temperature) for all Franck–Condon active normal modes. The initial wave packet  $\phi^{(0)}(\bar{x})$  is then Gaussian in shape. After the photoexcitation event, this initial wave packet evolves on an excited electronic surface. The evolution of this wave packet  $\phi(\bar{x}, t)$  can be computed by solving the equations of motion for the Gaussian parameters,<sup>3–5</sup> using as input excited state PES data. The electronic absorption spectrum is calculated using the well-known prescription<sup>3</sup>

$$\sigma(\omega_L) = \frac{Re}{\pi} \int_0^\infty dt \exp[i(\omega_L + E^{(0)})t] \langle \phi^{(0)} | \phi(t) \rangle \quad (7)$$

where  $\omega_L$  is the frequency of the laser beam and  $E^{(0)}$  is the vibrational energy eigenvalue corresponding to  $\phi^{(0)}$ . The equation for the emission spectrum is similar with reversal of the roles played by ground and excited electronic states and the change  $\omega_L \rightarrow -\omega_L$ .

We use the GWD technique to propagate the nuclear wave packets associated with the octatetraene molecule. These wave packets evolve on the anharmonic potential surfaces generated by QCFF/PI. For the absorption spectrum the initial wave packet is written as a product of the ground vibrational eigenfunctions associated with the normal modes of the ground electronic state of the molecule. For the emission spectrum, the ground vibrational eigenfunctions for the first excited state,  $2^1A_g$ , are used. At  $t = 0$  this initial wave packet is placed on the second excited state (absorption) or the ground state (emission) and evolved there. At every time step, the potential energy and appropriate derivatives of the PES at the center of the wave packet are evaluated via QCFF/PI (on the fly dynamics). For the systems studied in this paper, the FGA and TGA produced essentially identical results. Time evolution was carried out for 100 fs for each solvent configuration and the spectra were collected and averaged for the different configurations. We obtained converged static averages for the condensed phase spectra using 150–200 solvent configurations.

We executed the programs on a DEC  $\alpha$  workstation. It took several days to get the set of solvent configurations using AMBER, and 1 h to compute the nuclear wave packet evolution using QCFF/PI.

### 3. Results

The electronic spectroscopy of all-*trans*-1,3,5,7-octatetraene has been studied theoretically<sup>23</sup> and experimentally.<sup>19–21</sup> The absorption spectrum of this molecule involves an electronic transition from a ground state with  $A_g$  symmetry to the second lowest excited singlet state with  $B_u$  symmetry. The emission spectrum in the gas phase involves a transition between the same two states, and hence appears as a mirror image of the corresponding absorption spectrum. However, in the condensed phase the observed emission spectrum is due to a forbidden transition from the lowest excited singlet state with  $A_g$  symmetry. The energy gap between these first excited states of octatetraene is  $6400 \text{ cm}^{-1}$ .

The absorption and emission spectra of all-*trans*-1,3,5,7-octatetraene in the gas phase shows Franck–Condon structure arising from single and double bond C–C stretches (at  $1645$  and  $1235 \text{ cm}^{-1}$ , respectively).<sup>20</sup> Gavin et al.<sup>20</sup> also obtained experimental absorption and emission spectra of octatetraene in 10 different solvents. They observed that the absorption and emission spectra in solution are broad and some vibrational

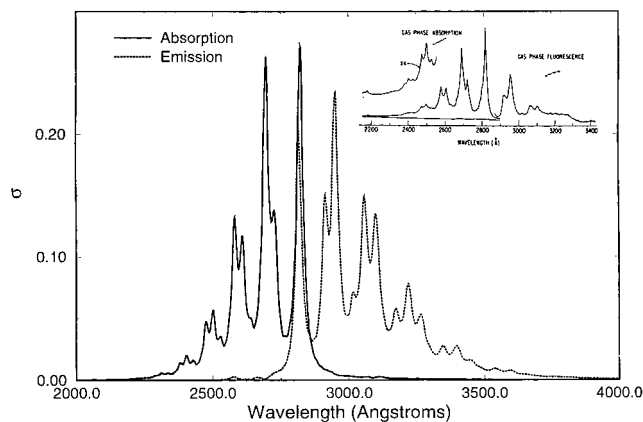


**Figure 1.** Calculated absorption and emission spectra of all *trans*-octatetraene in the gas phase computed via Gaussian wave packet dynamics and QCFF/PI electronic structure is shown in the main panel. The inset shows both experimental spectra.<sup>20</sup>

structure is apparent in the absorption spectrum. They noted that these spectra do not change in shape from solvent to solvent but the overall spectral band shifts in frequency. They also noticed a large energy gap that separates the absorption and emission spectra for a given solvent due to the different electronic states involved in the two processes.

We have chosen two solvents (chloroform and methanol) to test the sensitivity of our method. Experimentally,<sup>20</sup> the 0–0 absorption band of octatetraene in chloroform and methanol is red-shifted with respect to the gas phase band (by  $2973$  and  $2333 \text{ cm}^{-1}$ , respectively).

Figure 1 shows the absorption and emission spectra of octatetraene in the gas phase calculated using QCFF/PI plus GWD techniques. (In order to mimic instrumental broadening in the experimental gas phase measurements, we invoked an additional exponential damping factor in the integrand of eq 7. That is, in eq 7,  $E^{(0)} \rightarrow E^{(0)} + i\Gamma$ . A numerical value of  $\Gamma = 160 \text{ cm}^{-1}$  was employed.) The similarity between the calculated absorption spectrum and the experimental result<sup>20</sup> (shown in the inset of the figure) indicates that the combination of QCFF/PI electronic structure and GWD wave packet propagation is accurate enough to compute vibrationally resolved Franck–Condon spectra for this system. The calculated emission spectrum is almost a mirror image of the calculated absorption spectrum, consistent with the experimental situation. (The presence of resonance fluorescence prevented an accurate emission spectrum near the 0–0 region from being measured experimentally.) In Figure 2 we show the absorption spectrum calculated for octatetraene in the gas phase and in liquid chloroform at room temperature. (For the condensed phase spectra shown in Figures 2–4, no artificial correlation function damping was imposed.) Both are similar to the corresponding experimental spectra<sup>20</sup> (cf. insets of Figures 1 and 3). Interaction with the solvent broadens the spectrum of the solute molecule and shifts the calculated spectrum to the red by about  $2500 \text{ cm}^{-1}$ , in reasonable agreement with the experimental result of  $2973 \text{ cm}^{-1}$ . In Figure 3 we show the absorption and emission spectra of octatetraene in chloroform. The excited states involved in these two spectroscopic signatures are different, as noted above. This explains the energy gap between the origins of the two spectra. The calculated energy gap is about  $1200 \text{ cm}^{-1}$  higher than the experimental one. This difference may be caused in part by the different level of electronic structure theory used in QCFF/PI to calculate the electronic states involved in the two transitions. A comparison of these spectra with the corresponding experimental results (see inset to Figure 3) reveals good

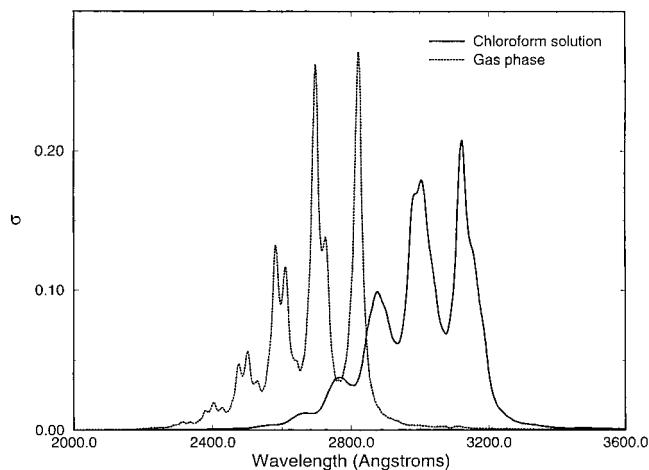


**Figure 2.** Calculated absorption spectra of all *trans*-octatetraene in chloroform solution at room temperature and in the gas phase. (The corresponding experimental spectra are presented in the insets to Figures 1 and 3.)

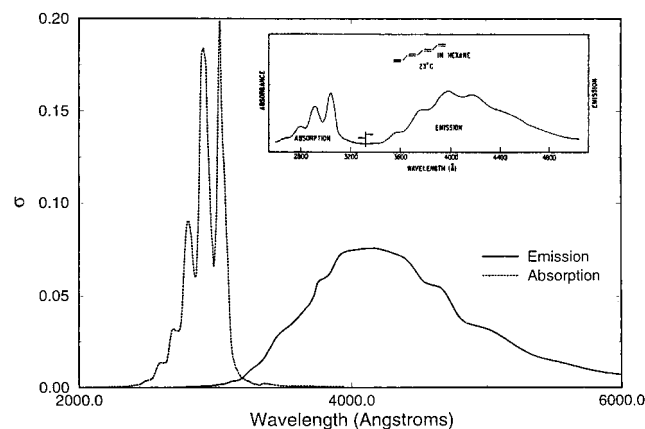


**Figure 3.** Calculated emission and absorption spectra of *trans*-octatetraene in chloroform solution at room temperature. The inset shows the corresponding experimental spectra in a hexane solution.<sup>20</sup> The experimental spectra in both solvents have similar shape but the 0–0 absorption band in chloroform is shifted 550  $\text{cm}^{-1}$  to the red compared with the one for hexane and the fluorescence maximum in chloroform is shifted 190  $\text{cm}^{-1}$  to the red compared with the maximum for hexane.<sup>20</sup>

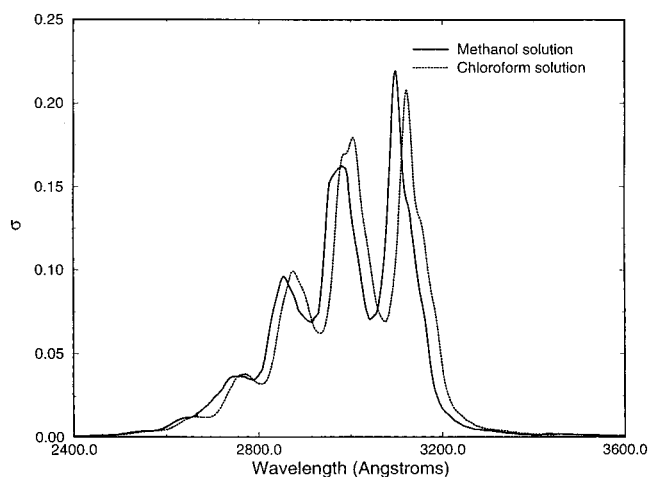


**Figure 4.** Calculated absorption spectra of *trans*-octatetraene in methanol and chloroform solutions at room temperature.

general agreement. Our emission spectrum is about 180 Å broader than the experimental one but it clearly reproduces the

loss of vibrational structure compared to the corresponding absorption spectrum.

To test the sensitivity of our method to changes in solvent environments, we show in Figure 4 the calculated absorption spectra of octatetraene in methanol and in chloroform at room temperature. It has been observed experimentally that the absorption spectrum of octatetraene does not change much in shape from solvent to solvent, but the overall absorption band shifts in frequency.<sup>20</sup> The absorption spectra we obtain indeed have similar shape and they are shifted to the red compared with the gas phase spectrum. The absorption spectrum in methanol is shifted to the blue compared with the spectrum in chloroform by about 450  $\text{cm}^{-1}$ . The experimental shift is 640  $\text{cm}^{-1}$ , in reasonable agreement with the result obtained in our computation. This provides evidence that the technique utilized here can be used to study a wide range of solvent–solute systems that show vibrational signatures in their Franck–Condon spectra. The quality of the results can vary depending on such factors as the accuracy of the electronic structure program that calculates the potential energy surfaces associated with the solute molecule and the degree of anharmonicity of the potential energy surfaces. However, due to the short-time nature of the associated dynamics (the condensed phase wave packet correlation functions calculated in the present work decayed irreversibly to zero in <60 fs), the method described in this paper should yield accurate results for many systems of chemical interest. The use of fast GWD techniques to propagate nuclear wave packets using potential surfaces evaluated on the fly via semiempirical electronic structure calculations (utilizing a spectroscopically calibrated ES program) will allow the use of this technique to study spectroscopic signatures for solutes with higher dimensionality than octatetraene (e.g., organic dyes that are commonly used in laser devices<sup>30</sup>).

#### 4. Concluding Remarks

We have developed a methodology that uses Gaussian wave packet techniques to propagate the nuclear coordinate wave packets associated with a polyatomic molecular system on instantaneous potential energy surfaces generated on the fly by an appropriate electronic structure program. These potential surfaces can incorporate interactions between the molecule and the surrounding environment. We have applied this algorithm to study the one-photon absorption and emission spectra of *all-trans*-1,3,5,7-octatetraene in the gas phase and in polar liquid solvents (specifically, chloroform and methanol). Comparison with experimental results shows that the technique is accurate enough to reproduce the main solvent-induced perturbations in the spectroscopic signals studied. The relatively small deviations of our computations compared to the experimental results can be attributed to the approximations inherent in the semiempirical QCFF/PI procedure and the force fields determining solvent–solvent and solute–solvent interactions, and the use of the “static limit” approximation for the effect of the solvent on the nuclear wave packet dynamics. Our results suggest that the methodology can be applied to other problems involving short-time quantum dynamics of condensed phase systems. These systems are not limited to solutes immersed in liquid solvents, but include, for example, molecular adsorbates on solid surfaces<sup>31</sup> and photo-dissociation dynamics of small molecules bound to biomolecules.<sup>32</sup>

We note in concluding that there has been a recent resurgence of interest in computing nuclear coordinate wave packet evolution via methods founded upon the initial value representation (IVR) of the van Vleck time-dependent semiclassical (SC)

propagator.<sup>33,34</sup> The intrinsic accuracy of the SC propagator appears to be very high.<sup>15</sup> Its evaluation for high-dimensional systems is not completely straightforward and is still under investigation.<sup>16–18</sup> Nevertheless, all IVR methods for evaluating the SC propagator use the same elementary ingredient found in simple Gaussian wave packet dynamics (GWD), namely a classical trajectory is propagated (based on specified initial values of position and momentum) and the second derivative matrix of the potential energy function (the Hessian matrix) is evaluated along the trajectory. In GWD this needs to be done only once to propagate an initially Gaussian wave packet, whereas in IVR-SC propagator methods, many trajectories (and the associated Hessian matrices) have to be propagated. The method developed here can thus be employed without essential modification in IVR-SC schemes in situations where the simple GWD approximation is inadequate. Since each classical trajectory is independent of all the others, it should be possible to employ parallel processing computer platforms to relieve the burden of having to evolve many trajectories in order to propagate one nuclear coordinate wave packet.

**Acknowledgment.** This work was supported by NSF grant CHE9529674. A.E.C. thanks the Andrew D. Mellon Committee for support through a Mellon Predoctoral Fellowship at the University of Pittsburgh. We also thank Profs. P. R. Callis and F. Zerbetto for providing us with updated versions of the QCFF/PI program and for helpful discussions.

## References and Notes

- (1) For a cross section of recent developments in methods for quantum wave packet dynamics and molecular electronic structure, consult: *Encyclopedia of Computational Chemistry*; Schleyer, P. v. R., Allinger, N. L., Clark, T., Gasteiger, J., Kollman, P. A., Schaefer III, H. F., Schreiner, P. R., Eds.; John Wiley & Sons: Chichester, UK; 1998.
- (2) Carr, R.; Parrinello, M. *Phys. Rev. Lett.* **1985**, *55*, 2471.
- (3) Heller, E. J. *Acc. Chem. Res.* **1981**, *14*, 368.
- (4) Heller, E. J. *J. Chem. Phys.* **1975**, *62*, 1544.
- (5) Heller, E. J. *J. Chem. Phys.* **1981**, *75*, 2923.
- (6) Martinez et al. have propagated frozen Gaussian wave packets based on force fields obtained from ab initio electronic structure calculations performed on the fly,<sup>7</sup> but not for excited state spectroscopy and not for condensed phase systems.
- (7) Martinez, T. J.; Levine, R. D. *Chem. Phys. Lett.* **1996**, *259*, 252. Martinez, T. J.; Levine, R. D. *J. Chem. Phys.* **1996**, *105*, 6334. Martinez, T. J. *Chem. Phys. Lett.* **1997**, *272*, 139. Ben-Nun, M.; Martinez, T. J. *Chem. Phys. Lett.* **1998**, *298*, 57. Thompson, K.; Martinez, T. J. *J. Chem. Phys.* **1999**, *110*, 1376.
- (8) If the potential energy surface is at most quadratic in the nuclear coordinates, then Gaussian wave packet dynamics is exact for all times.
- (9) Neria, E.; Nitzan, A. *J. Chem. Phys.* **1993**, *99*, 1109; *Chem. Phys.* **1994**, *183*, 351.
- (10) Kulander, K.; Heller, E. J. *J. Chem. Phys.* **1978**, *69*, 2439. Drolshagen, G.; Heller, E. J. *J. Chem. Phys.* **1983**, *79*, 4005. Drolshagen, G.; Heller, E. J. *Surf. Sci.* **1984**, *139*, 260.
- (11) Coalson, R. D.; Karplus, M. *J. Chem. Phys.* **1990**, *93*, 3919.
- (12) Messina, M.; Coalson, R. D. *J. Chem. Phys.* **1990**, *92*, 5712. Messina, M.; Coalson, R. D. *J. Chem. Phys.* **1991**, *95*, 5364. Messina, M.; Coalson, R. D. *J. Chem. Phys.* **1991**, *95*, 8977.
- (13) Braun M.; Metiu, H.; Engel, V. *J. Chem. Phys.* **1998**, *108*, 8983.
- (14) Gaussian wave packet dynamics is a simple example of a time-dependent semiclassical wave packet propagation technique. More sophisticated semiclassical propagation schemes have been developed which yield longer-time accuracy on anharmonic potential surfaces.<sup>15–18</sup> The “cost” of this improved performance is the need to independently propagate a large set of Gaussians instead of a single one as required by GWD. Thus the method proposed in this work for propagating a single Gaussian wave packet can be used to propagate swarms of Gaussians as required in the more sophisticated schemes. This point is discussed further in the Concluding Remarks.
- (15) Heller, E. J. *J. Chem. Phys.* **1991**, *94*, 2723.
- (16) Sun, X.; Miller, W. H. *J. Chem. Phys.* **1997**, *106*, 6346; **1998**, *108*, 8870.
- (17) Herman, M. F.; Kluk, E. *Chem. Phys.* **1984**, *91*, 27. Kluk, E.; Herman, M. F.; Davis, H. L. *J. Chem. Phys.* **1986**, *84*, 326.
- (18) Ovchinnikov, M.; Apkarian, V. A. *J. Chem. Phys.* **1998**, *105*, 10312.
- (19) Kohler, B. E.; Spiglanin, T. A.; Hemley, R. J.; Karplus, M. *J. Chem. Phys.* **1984**, *80*, 23.
- (20) Gavin Jr., R. M.; Weisman, C.; McVey, J. K.; Rice, S. A. *J. Chem. Phys.* **1978**, *68*, 522.
- (21) Heimbrock, L. A.; Kenny, J. E.; Kohler, B. E.; Scott, G. W. *J. Chem. Phys.* **1981**, *75*, 4338.
- (22) Warshel, A.; Karplus, M. *J. Am. Chem. Soc.* **1972**, *94*, 5612; Warshel, A. *Isr. J. Chem.* **1973**, *11*, 709.
- (23) Orlandi, G.; Zerbetto, F.; Zgierski, M. Z. *Chem. Rev.* **1991**, *91*, 867. Zerbetto, F.; Zgierski, M. Z.; Negri, F.; Orlandi, G. *J. Chem. Phys.* **1988**, *89*, 3681.
- (24) Muino, P. L.; Callis, P. R. *J. Chem. Phys.* **1994**, *100*, 4093.
- (25) Broo, A.; Pearl, G.; Zerner, M. C. *J. Phys. Chem. A* **1997**, *101*, 2478.
- (26) Roothaan, C. C. J. *J. Chem. Phys.* **1951**, *19*, 1445.
- (27) Pearlman, D. A.; Case, D. A.; Caldwell, J. W.; Ross, W. S.; Cheatham III, T. E.; Ferguson, D. M.; Seibel, G. L.; Chandra Singh, U.; Weiner, P. K.; Kollman, P. A. *AMBER 4.1*, University of California, San Francisco, 1995.
- (28) Cornell, W. D.; Cieplak, P.; Bayly, C. I.; Gould, I. R.; Merz Jr., K. M.; Ferguson, D. M.; Spellmeyer, D. C.; Fox, T.; Caldwell, J. W.; Kollman, P. A. *J. Am. Chem. Soc.* **1995**, *117*, 5179.
- (29) Eksterowicz, J. E.; Miller, J. L.; Kollman, P. A. *J. Phys. Chem. B* **1997**, *101*, 10971.
- (30) Grofcsik, A.; Kubinyi, M.; Jones, W. J. *J. Mol. Struct.* **1995**, *348*, 197. Hasche, T.; Ashworth, S. H.; Riedle, E.; Woerner, M.; Elsaesser, T. *Chem. Phys. Lett.* **1995**, *244*, 164. Ashworth, S. H.; Hasche, T.; Woerner, M.; Riedle, E.; Elsaesser, T. *J. Chem. Phys.* **1996**, *104*, 5761.
- (31) Harrison, I.; Polanyi, J. C.; Young, P. A. *J. Chem. Phys.* **1988**, *89*, 1475.
- (32) Mohny, B. K.; Wang, C.; Walker, G. C. *Abstr. Pap. Am. Chem. Soc.* **1998**, *216*, U779.
- (33) Van Vleck, J. H. *Proc. Nat. Acad. Sci.* **1928**, *14*, 178.
- (34) Miller, W. H. *Adv. Chem. Phys.* **1974**, *25*, 69.